Connection Between Regge Behavior and Fixed-Angle Scattering*

R. Blankenbecler and S. J. Brodsky
Stanford Linear Accelerator Center, Stanford University, Stanford, California 94305

J. F. Gunion†
Massachusetts Institute of Technology, Cambridge, Massachusetts 02139

R. Savit‡
Stanford Linear Accelerator Center, Stanford University, Stanford, California 94305
(Received 27 August 1973)

The physical origins and dynamical details of Regge behavior are studied by examining a general class of theories which are capable of describing the observed *large*-momentum-transfer data and extending them into the intermediate-t range. The mechanism responsible for the smooth connection between the deep-scattering region and the Regge region is discussed in detail. We derive a convenient new form of the exact integral equation which describes generalized ladder graphs containing irreducible scattering amplitudes as the rungs. The limiting behavior of the Regge trajectories and residues are then calculated in both the single-channel and the more realistic coupled-channel cases. The trajectories are found to approach negative constants for large negative momentum transfer and the residues fall as powers in the same limit. Furthermore, since the forward and backward Regge regimes must join smoothly onto the same fixed-angle behavior, there are relations between *a priori* unrelated trajectory functions and residues. The standard properties of Regge poles, in particular factorization and signature, are shown to be present even though the basic, fixed-angle interaction possesses neither of these properties. These general considerations are then applied to the more specific constituent-interchange model. Here we find that the asymptotic behavior of the trajectories and residues are controlled by the form factors of the particles involved in the scattering. Finally, we elucidate the relationship between the constituent-interchange diagrams and the Harari-Rosner duality diagrams.

I. INTRODUCTION

The conventional wisdom of Regge analyses states that hadron scattering at large angles is hopelessly complicated; one could never hope to unravel the effects of cuts, nonleading trajectories, and other secondary singularities of the j plane as they become increasingly important and intertwined as $|t|$ and $|u|$ become large. In this paper we present just the opposite view: Regge behavior at large $|t|$ and large $|u|$ is elegant and simple; moreover, scattering in this region directly reflects the fundamental properties of the interacting hadrons at short distances.

The most dramatic feature of this new point of view for Regge theory is that all trajectories, $\alpha_i(t)$, in hadron-hadron scattering will approach negative constants as $t \to -\infty$. (A logarithmic behavior is also possible and is not inconsistent with our approach.) For instance, in a model calculation we find that meson-meson and meson-baryon scattering is controlled at large angles by four factorizable Regge poles which become degenerate and approach ≈ -1 as $t \to -\infty$. In baryon-baryon scattering, the contributions of these four trajectories cancel as $|t|$ becomes large, thereby exposing a nonleading set of approximately exchange-degenerate trajectories which approach ≈ -3 at $t \to -\infty$. The dependence of the residues and, most important, the behavior of the first-order deviation of the trajectories from their asymptotic values can be readily obtained. Thus we can discuss quantitatively the *transition* region which connects the large-angle asymptotic region of deep-elastic scattering ($t/s, u/s$ fixed; $s \to \infty$) to the multiparticle coherent Regge regions of fixed t or u.

The simplest illustration of this type of Regge behavior is found in superrenormalizable field theories such as ϕ^3. As is well known, the t-channel iteration of the Born amplitude, e.g., $K(s,t) = g^2/(s - m^2 + i\epsilon)^{-1}$, generates Regge behavior. However, for large $|t|$, the leading behavior of the complete amplitude is given by the Born term and thus the effective trajectory $\alpha(t)$ approaches -1.

In the calculations presented here we start with simple forms for the Born term K, which will reproduce the features of all current large-angle scattering data. The t-channel iteration of this basic interaction then yields moving trajectories, $\alpha_i(t)$. Iterations in the s channel which unitarize the theory become important at low energies (in the resonance region) and at high energies when an $\alpha(t)$ approaches $+1$, which is expected to occur

only at small values of $|t|$. Thus our simple theory should apply, except near $|t| \sim 0$, where the above complications are manifest.

Because of the power-law nature of the assumed Born amplitudes, one finds that the leading behavior of the complete amplitude in the deep-scattering region is given by the Born terms, and the asymptotic trajectories and residues are thereby constrained to produce this behavior. In the asymptotic large-angle region, the interaction time is so short that only the simplest "hadron irreducible" interactions can take place, and the use of the impulse approximation is justified. In this region the coherent Regge effects are suppressed, exposing the basic mechanisms which underlie the interactions between hadrons.

It should be noted that our conclusions concerning the nature of Regge behavior in the large-angle and transition regions are independent of any model used for calculating the basic interaction so long as the underlying theory allows t-channel iterations. Indeed, we could almost rely solely on experimental data for the behavior in the large-angle region. We admit our prejudices, however, in favor of the parton-interchange model discussed in Refs. 1, 2, and 3, since this theory is a natural consequence of composite hadron models and correctly reproduces the deep-scattering exclusive data—given only the power-law falloff of the meson and baryon form factors. We can also consistently allow for logarithmic modifications of the basic power-law results.

It is possible, of course, that other mechanisms such as vector-meson exchange,[4] elementary gluon exchange,[5] direct parton-parton interactions,[6] or perhaps hadronic bootstrap mechanisms,[7] could contribute to the Born terms. However, in view of the apparent success of the interchange model, the coupling constant between these other mechanisms and the real hadronic world may well be small. In that case, it is clear that as one approaches the region of small $|t|$ or $|u|$ from the deep-scattering region, the first corrections to simple interchange results will be those due to mulitple interactions of the basic interchange mechanism itself. Such iterative effects Reggeize the scattering process when the forward or backward regions of exclusive scattering are approached, and other interactions will only become important at quite small $|t|$, where coherence can overcome their intrinsically small coupling constant. Furthermore, if such additional mechanisms exist, it will be important to know the kernel outside the deep region in order to extend the Reggeization procedure to the kinematic domain of very small $|u|$ or $|t|$. However, we want to emphasize that, the discussion of this paragraph notwithstanding, the approach of the present paper is not tied to a specific model of deep scattering.

Physically, the inclusion of multiple interactions in the t channel can be thought of as allowing one of the incoming hadrons produce in a *bremsstrahlung* process a secondary hadron which, in turn, undergoes the basic interaction with the other incoming hadron, at a lower effective energy. The resulting theory has the complexities of normal Regge behavior in the forward and backward regions and joins smoothly to the impulse result in the deep region. The physical consequences and effects of the hadronic bremsstrahlung component on parton-model results, especially in electromagnetic processes, are discussed in another paper.[8]

The outline of this paper is as follows. In Sec. II we derive a very convenient three-dimensional Euclidean integral equation for the iteration of two-body scattering amplitudes. An alternate derivation using time-ordered perturbation theory in the infinite-momentum frame is given in an Appendix to help in clarifying the physics of the equation.

In Sec. III we review the well-known fact that the iteration of the ladder Born terms, K, in the t channel becomes important and leads to Regge behavior of the scattering amplitude when the backward or forward regions of exclusive scattering are approached.

In Sec. IV, a treatment of more complicated basic interactions is given. The Born terms used here provide a realistic description of large-angle scattering data. The single- and coupled-channel cases, as well as the effects of signature, are discussed, and the transition region between the fixed-angle and the fixed-t or Regge domain is described in detail. Techniques applicable to meson and baryon scattering in the large-angle and transition regions are also presented.

II. DERIVATION OF THE INTEGRAL EQUATION

In this section we shall derive a very useful three-dimensional integral equation which gives the convolution of two general, two-particle scattering amplitudes: $M = K \times T$. Each amplitude K and T can have general off-mass-shell dependence on its external legs. Upon integration over the mass squared l^2 of the Feynman loop, a covariant equation is obtained in terms of the transverse momentum and fractional longitudinal momentum variables familiar from infinite-momentum frame and light-cone variable analyses.

Among the uses of this equation are the following:

(1) If K is chosen as a kernel which fits large-angle scattering, then the t-channel iteration of

K, i.e., $M=K+K\times M$ will produce an integral equation which determines M in terms of K. This equation yields Regge behavior and provides a description of the physics of the transition between fixed angle and fixed t. This problem is discussed in detail in Sec. III.

(2) If $K=K_\gamma$ is taken as a basic (e.g., parton model) Compton or electroproduction (or weak production) amplitude, then the convolution $M_\gamma=K_\gamma+K_\gamma\times M$, with a sum of hadronic scattering amplitudes M, provides the synthesis between electromagnetic parton models and hadronic physics. The Regge behavior of the Compton electroproduction amplitude in both energy and the Bjorken scaling variable ω is a natural reflection of the Regge behavior of the hadronic amplitude, M. This will be discussed in detail in another paper.[8]

(3) Since K is by definition irreducible with respect to two-hadron particle states in the t channel, Regge behavior in M can be viewed as arising from the elementary scattering on the "hadronic bremsstrahlung" constituents of the target. The spectrum of the hadronic bremsstrahlung is Regge-behaved, $G(x)dx\sim x^{-\alpha}dx$ for $x\sim 0$ ($\alpha\cong 1$ for Pomeron behavior), where x is the fractional longitudinal momentum in the $P\to\infty$ frame. Further discussion of this point may be found in Ref. 8. This picture is similar to the "wee"-parton-exchange theory of Feynman[9] except that *hadrons* rather than partons with $x\sim 0$ are responsible for Regge behavior in hadron-hadron scattering.

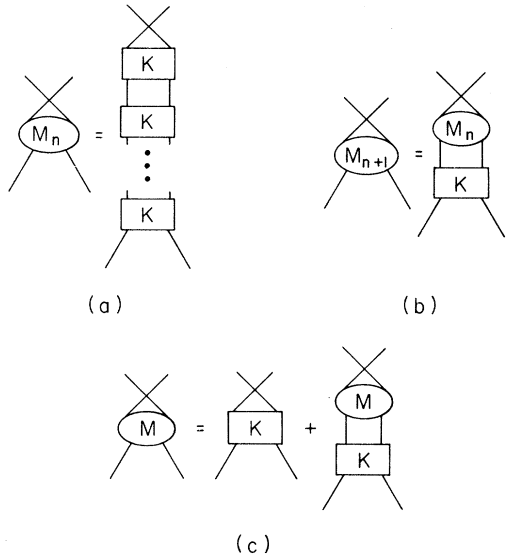

FIG. 1. The integral equation for an hadronic amplitude generated by the t-channel iteration of an hadronic scattering kernel, K. (a) The amplitude in nth order. (b) The iteration equation computed in Eq. (6). (c) The integral equation derived in Eq. (10).

The derivation of the integral equation presented below will use a method discussed by Chang and Ma[10] and Schmidt[11] in which a covariant Feynman expression is transformed to a three-dimensional form in terms of light-cone variables. An alternative derivation using time-ordered perturbation theory in the infinite-momentum frame also can be carried out. Although somewhat more cumbersome, this latter derivation can be very illuminating, especially in the context of constituent models and in comparison with earlier calculations. It is discussed in detail in the Appendix.

Let us begin by considering a diagram of the type shown in Fig. 1(a). This figure describes a term M_n which is the n-fold iteration in the t channel of some basic scattering amplitude K. The total scattering amplitude is a sum over n,

$$M=K+\sum_{n=1}^{\infty}M_n\ . \tag{1}$$

In order to discuss the properties of the sum, it is convenient to derive an integral equation for M. First, a recursion relation for M_{n+1} in terms of M_n and K will be derived as depicted in Fig. 1(b). If all particles are spinless, covariant perturbation theory yields the expression

$$M_{n+1}(u,t;\nu^2,\tilde{\nu}^2)=\int\frac{d^4l}{(2\pi)^4 i}\left[l^2-m^2+i\epsilon\right]^{-1}\left[(l+q)^2-m^2+i\epsilon\right]^{-1}\times K(\tilde{u},t;\nu^2,\tilde{\nu}^2;l^2,(l+q)^2)M_n(\bar{u},t;l^2,(l+q)^2)\ , \tag{2}$$

where $u=(p-r)^2$, $t=q^2$, $\bar{u}=(l-r)^2$, $\tilde{u}=(p-l)^2$, $\nu^2=p^2$, $\tilde{\nu}^2=(p+q)^2$. The dependence of M_n on the upper masses r^2 and $(q+r)^2$ has been suppressed but the other off-mass-shell dependences of M_n and K have been explicitly displayed.

It is convenient at this point to introduce a dispersion representation for K:

$$K(\tilde{u},t;\nu^2,\tilde{\nu}^2;\lambda^2,\tilde{\lambda}^2)=\int\frac{d\sigma^2}{(\sigma^2-\tilde{u}+i\epsilon)}\times W(\sigma^2,t;\nu^2,\tilde{\nu}^2;\lambda^2,\tilde{\lambda}^2), \tag{3}$$

where W is the discontinuity of K across the $\tilde{u}$ cut and the notation $\lambda^2=l^2$, $\tilde{\lambda}^2=(l+q)^2$ has been introduced. When this expression is introduced into Eq. (2), the integrand depends on l through the three explicit propagators, as well as through the dependence of M_n on $\bar{u}=(l-r)^2$ and the off-mass-shell dependences $(\lambda^2,\tilde{\lambda}^2)$ of M_n and W.

The integration over l^2 can, however, be readily carried out. To do this conveniently, we choose the following parameterization of the Lorentz frame:

$$p=\left(P+\frac{\nu^2}{4P},\vec{0}_\perp,P-\frac{\nu^2}{4P}\right),\quad q=\left(\frac{q\cdot p}{2P},\vec{q}_\perp,-\frac{q\cdot p}{2P}\right),$$
$$l=\left(xP+\frac{l^2+\vec{l}_\perp^{\,2}}{4xP},\vec{l}_\perp,xP-\frac{l^2+\vec{l}_\perp^{\,2}}{4xP}\right),\tag{4}$$
$$r=\left(\frac{r\cdot p}{2P},\vec{r}_\perp,-\frac{r\cdot p}{2P}\right).$$

The rapidity of the incident particle p_μ is $\ln(2P/\nu)$, and is, of course, arbitrary. The choice $P=\nu/2$ is the lab system, and the choice $P\to\infty$ is the usual infinite-momentum frame. In this case $x\equiv(l_0+l_3)/2P$ can be identified with the fractional longitudinal momentum l_3/p_3. Note that the masses of the two external particles at the top, $r^2=-r_\perp^{\,2}$ and $(r+q)^2=-(r+q)_\perp^{\,2}$, have been chosen to be spacelike. This choice produces many simplifications which will become apparent as we proceed. It will be simple to continue our final results back to stable physical-mass values at the end of the calculation.

To obtain the recursion relation in its most useful form, the l^2 integration must be explicitly performed. Using the above parameterization of l, one finds (independent of P) that[12]

$$\int d^4l=\int_{-\infty}^{\infty}\frac{dx}{2|x|}\int d^2l_\perp\int dl^2.\tag{5}$$

The obvious poles in l^2 arise from the three explicit propagators and the u dependence of M_n (which can be written in the form of a dispersion relation). The additional singularities in l^2 which may arise as a result of the off-mass-shell dependences of the subamplitudes will be discussed below. Using the four-vectors as given in (4), it is easy to see that all these singularities are in the lower half l^2 plane if x is outside the range (0, 1). If x is inside this range, only the pole at $(p-l)^2=\sigma^2-i\epsilon$ is in the upper half plane and the l^2 integration can be immediately performed to yield

$$M_{n+1}(u,t;\nu^2,\tilde{\nu}^2)=\int\frac{d^2l_\perp d\sigma^2}{2(2\pi)^3}\times\int_0^1\frac{dx}{(1-x)}\frac{M_n(\bar{u},t;\nu^2;\lambda^2,\tilde{\lambda}^2)W(\sigma^2,t;\lambda^2,\tilde{\lambda}^2)}{(\lambda^2-m^2)(\tilde{\lambda}^2-m^2)},\tag{6}$$

where

$$\lambda^2-m^2=x[\nu^2-S(\vec{l}_\perp,x)]\equiv xD_i\,,$$
$$\tilde{\lambda}^2-m^2=x[\tilde{\nu}^2-S(\vec{l}_\perp+(1-x)\vec{q}_\perp,x)]\equiv xD_f\,,\tag{7}$$

$$\bar{u}-m^2=x[u-S(\vec{l}_\perp-(1-x)\vec{r}_\perp,x)]\,,\tag{8}$$

and

$$S(l_\perp,x)\equiv\frac{l_\perp^{\,2}+m^2}{x}+\frac{l_\perp^{\,2}+\sigma^2}{1-x}\,,\tag{9}$$

which is the sum of the kinetic energies in the infinite-momentum frame time-ordered analysis.

A few comments about this result are useful here. First, the fact that only values of x in the range (0, 1) contribute to the integral is due to the choice of a particular type of frame. Using the infinite-momentum method language, the vectors r and $q+r$ are not allowed to bring in any longitudinal momentum (in the $P\to\infty$ limit). This is accomplished by giving the masses r^2 and $(q+r)^2$ spacelike values. This statement is identical to the observation made in the Appendix that only one time-ordered graph contributes because the longitudinal momentum must flow to the right in each line.

Second, we note that the integral in Eq. (6) looks very much like those that appear in time-ordered perturbation theory in the infinite-momentum frame. In fact, if a spectral representation of M_n is introduced similar to that given for K in Eq. (3) and is inserted into (6), the result is exactly the time-ordered perturbation theory expression for the box graph [with external masses ν^2, $\tilde{\nu}^2$, $-r_\perp^{\,2}$, and $-(q+r)_\perp^{\,2}$] multiplied by weight functions and integrated over the masses of the rungs.

Third, in the case of simple analytic off-shell behavior for K (e.g., Born terms with vertex parts), Eq. (6) may be used in a straightforward way. In the case of other, more complicated graphs involving certain kinds of singularities in λ^2 and $\tilde{\lambda}^2$, the σ^2 line integration must be deformed to avoid singularities of the integrand.[13] This more complicated situation does not occur in the calculation of the absorptive part of M, nor in any of the examples treated in this paper.

Having demonstrated the recursion relation given by Eq. (6), the last (trivial) step in deriving an integral equation for M is to sum over n. The result is

$$M(u,t;\nu^2,\tilde{\nu}^2)=K(u,t;\nu^2,\tilde{\nu}^2)+\int\frac{d^2l d\sigma^2}{2(2\pi)^3}\int_0^1\frac{dx\,M(\bar{u},t;\lambda^2,\tilde{\lambda}^2)}{x^2(1-x)D_iD_f}\times W(\sigma^2,t;\nu^2,\tilde{\nu}^2,\lambda^2,\tilde{\lambda}^2),\tag{10}$$

where the D's are defined by Eq. (7). The structure of the formula is depicted in Fig. 1(c). This is a particularly simple and convenient equation to use to discuss Reggeization since it is covariant yet has a nonsingular, Euclidean kernel.

III. REGGE BEHAVIOR IN LADDER APPROXIMATION

As a first application of the integral equation (10), we turn to a well-known problem, that of the Regge behavior of sums of simple ladder graphs. This example will illustrate in a straightforward way the transition between fixed-t and fixed-angle behavior.

We work in ϕ^3 theory, and choose as our Born term a u-channel pole,

$$K=-g^2(u-\mu^2+i\epsilon)^{-1}.$$

Using the dispersion representation (3), the weight function which corresponds to this kernel is

$$W(\sigma^2)=g^2\delta(\mu^2-\sigma^2).$$

Iterating this kernel in the t channel will generate simple ladder graphs (as shown, for example, in Fig. 2). Notice that the top two lines are crossed, making the graph nonplanar, and therefore purely real for $s>0$, $t<0$.[14]

Turning now to Eq. (10) we see that with the present choice for W, a power behavior for M is consistent with the integral equation. In particular, if one attempts to write M in the form

$$M=\beta(t;\nu^2,\tilde{\nu}^2)\left(\frac{m^2-u}{m^2}\right)^{\alpha(t)}+\cdots,$$

then for large $(-u)$, the equation for M becomes a nonsingular homogeneous equation for β if $\alpha(t)>-1$ and

$$\beta(t;\nu^2,\tilde{\nu}^2)=\frac{g^2}{2(2\pi)^3}\int_0^1 dx\int\frac{d^2l_\perp x^{\alpha(t)-1}}{(1-x)D_iD_f}\beta(t;\lambda^2,\tilde{\lambda}^2).$$

To discuss the transition from the large-$|t|$ to the small-$|t|$ region, let us examine the first two terms in the series for M, and consider a slightly more general case in which W may depend upon t. To second order in W, the scattering amplitude can be written as

$$M=\int d\sigma^2\frac{W(\sigma^2,t)}{\sigma^2-u}+\int\frac{d\sigma^2d\rho^2}{2(2\pi)^3}W(\sigma^2,t)W(\rho^2,t)J, \tag{11}$$

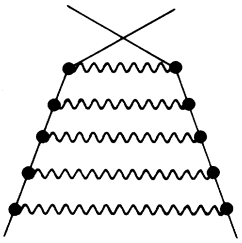

FIG. 2. Ladder graph generated in ϕ^3 theory. This is calculated explicitly in the Appendix.

where

$$J=\int d^2l_\perp\int_0^1\frac{dx}{x^2(1-x)D_iD_f(\rho^2-\bar{u})}. \tag{12}$$

If the three denominators are combined using Feynman parameters, the $d^2l_\perp$ integration can be performed and J becomes [after scaling the Feynman parameters by $(1-x)$],

$$J=\pi\int_0^1 dx\,dy\,d\beta_1d\beta_2\delta(1-x-y-\beta_1-\beta_2)\Delta^{-2},$$

where

$$\Delta=\{(1-x-y)m^2+\beta_1\beta_2q_\perp^2-xyu+y\rho^2+x\sigma^2-x(\beta_1\nu^2+\beta_2\tilde{\nu}^2)+y[\beta_1\vec{r}_\perp^{\,2}+\beta_2(\vec{q}_\perp+\vec{r}_\perp)^2]\}. \tag{13}$$

This form explicitly shows the analyticity in the upper masses and the symmetry under the double interchange $\nu^2\leftrightarrow-\vec{r}_\perp^{\,2}$ and $\tilde{\nu}^2\leftrightarrow-(\vec{q}_\perp+\vec{r}_\perp)^2$. This result could also have been obtained directly from a standard Feynman-parameterized form for M.

For large $(-u)$, the leading behavior in J arises from small values of x and y, and one easily finds from (13) or directly from (12) that

$$J\cong\frac{\pi}{(-u)}\ln\left(\frac{-u}{m^2}\right)\times\int_0^1 dz[m^2+z(1-z)\vec{q}_\perp^{\,2}]^{-1}+O(1/u), \tag{14}$$

and this leading behavior is essentially independent of σ^2 and ρ^2 and the external masses, and depends only on the internal mass m^2. Expanding the Regge expression for M,

$$M\sim\beta(t)(-u/\mu^2)^{\alpha(t)}$$

in powers of $\ln(-u)$, and comparing the first two terms with (11), we find that to lowest order in W,

$$\beta(t)=\int d\sigma^2W(\sigma^2,t)/\mu^2$$

and

$$\alpha(t)=-1+\frac{\beta(t)\mu^2}{4(2\pi)^2m^2}\int_0^1 dz[1-z(1-z)t/m^2]^{-1}. \tag{15}$$

In the simple ladder case we are considering, $\beta(t)$ is g^2/μ^2, to this order in the couplings, and $\alpha(t)$ in (15) reduces to the well-known result of Lee and Sawyer.[15] This is equivalent to a leading-log perturbation expansion[16] in the coupling g, and thus yields the result (15). Finally, for comparison with later results, we note that $\alpha(t)$ approaches its asymptotic limit for large $|t|$ as

$$\alpha(t)\sim-1+\frac{\mu^2}{2(2\pi)^2m^2}\frac{\beta(t)}{(-t)}\ln(-t/\mu^2)+\cdots. \tag{16}$$

Hence this simple ladder model yields the fol-

lowing physical picture of exclusive $2 \to 2$ scattering: In the deep, fixed-angle region, only the basic Born amplitude is important. Large-angle scattering, therefore, is particularly simple. As the forward or backward direction is approached, multirunged ladders become increasingly important, thus Reggeizing the underlying process and building up the energy dependence of the scattering amplitude.

To gain further insight into the relationship between the deep and Regge regions, it is very instructive to consider another simple example for the kernel in the iteration scheme. The graph we want to discuss is shown in Fig. 3: This kernel includes one vertex correction. We work in the frame described above and parameterize the additional momentum k as

$$k = \left(zP + \frac{k^2 + k_\perp^2}{4zP}, \vec{k}_\perp, zP - \frac{k^2 + k_\perp^2}{4zP} \right) .$$

Using this frame it is straightforward to carry out the dl^2 and dk^2 contour integrals. Doing this, we find there are three terms which contribute to the diagram. These are shown as time-ordered graphs in Fig. 4, where the dashed lines indicate which particles are on-mass-shell. The first term, Fig. 4(a) contributes when $z < x$, while the others contribute when $z > x$. Remember that in the infinite-momentum limit $P \to \infty$, z and x are the fractions of longitudinal momentum carried by the lines k and l, respectively.

We may now ask which of the vertex-correction time orderings we expect to dominate in the Regge region. Since, as we have discussed, small x is most important here, we expect the time orderings with $x < z$ will predominate. These are the graphs of Figs. 4(b) and 4(c). As we move away from the Regge region $|t|$ grows for fixed $|u|$, and, as we see from Eqs. (11)–(13), it becomes more and more important for α and β to be small in order to get a sizable contribution to J. Since the δ function must be satisfied, regions of the x integration, where x is not near zero, become increasingly important, and it is no longer justifiable to consider only contributions to J coming from small x. As far as the vertex-correction graphs are concerned this means that the time ordering of Fig. 4(a) becomes more and more important. In addition, when $|t|$ is large, all the amplitudes, M_n, $n > 0$ are down by a least a factor $|t|^{-1}$ from the Born term as we have shown. The picture of Regge behavior and its relation to deep scattering which emerges from these considerations is the following. In the t channel, the Regge region is dominated by the exchange of light particles with relatively small longitudinal momentum in the infinite-momentum frame (x near zero). If these particles are partons, we recover Feynman's idea that Regge behavior arises from the exchange of wee partons.[9] Notice, however, that the exchanged particles need not have pointlike form factors or unusual quantum numbers—in our formalism, the possibility that they are ordinary hadrons is more natural. Meanwhile, the picture in the s channel is that in each amplitude M_n, the Regge region is dominated by the many-particle intermediate states as in Figs. 4(b) and 4(c)—whatever particles there are want to live as long as possible. In addition, amplitudes M_n with increasingly large values of n become important in order to build up the moving Regge trajectory. As $|t|$ increases, each M_n gets larger and larger contributions from diagrams like Fig. 4(a)—that is, the particles in the intermediate state pull back and live for shorter and shorter times. Furthermore, as $|t|$ increases, all the amplitudes, M_n for $n > 0$ become small in comparison with the Born term by at least a factor of $|t|^{-1}$, until finally in the deep region only the Born term is important.

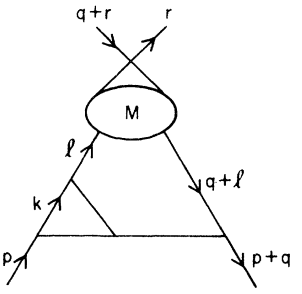

FIG. 3. Example of a vertex insertion in a ϕ^3 theory calculation of the full hadronic amplitude.

IV. THE TRANSITION BETWEEN THE DEEP AND THE REGGE REGIONS

In the simple example of Sec. III, we reviewed how the dynamics of scattering in the deep region (roughly, $s \to \infty$, t/s, u/s fixed; a more precise definition is given below) produces, by t-channel

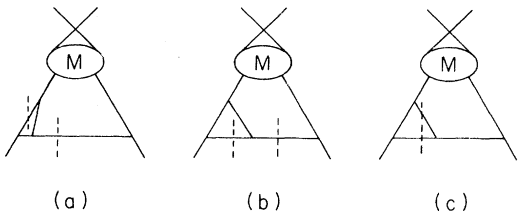

FIG. 4. Time-ordered contributions to the vertex insertion diagram of Fig. 3. The dashed lines indicate which intermediate-state particles are on the mass shell.

iteration, ladder amplitudes which are increasingly important as we move into the Regge regions. Iterations of this type build up moving Regge poles.

In this section we will extend the analysis of Sec. III to more realistic cases. The basic interaction kernels K which are used here provide a good description of the large-angle data. While their form is motivated by the parton-interchange model, the iterative contribution to Reggeization is more general and is not tied to any specific model for deep scattering.

Near the forward and backward directions, coherent effects, including multiple gluon exchange between the hadronic constituents, will very probably become important. These are not generated by the t-channel iteration procedure but must be included as an additional irreducible kernel. As $|t|$ becomes larger, such effects may be suppressed relative to iteration of the basic Born amplitude, provided the relevant coupling constants are small. This is certainly the case in the interchange theory of the deep-scattering (fixed-angle) region. In this theory the iterative contribution will provide an accurate picture of the nature of the transition between the d ›p-scattering region and the Regge region. Consideration of the coherent effects of gluon exchange is beyond the scope of the present paper. Indeed, if present, such direct interaction could be capable of binding the propagating intermediate constituents to form sets of hadrons or resonances, such as depicted in Fig. 5, in the appropriate kinematic region. In this picture the positive-energy portion of a trajectory probes different aspects of the underlying interactions than does the trajectory for large negative t.

In this section, therefore, we shall approximate the kernel in the iterative Reggeization process and neglect other types of two-hadron irreducible kernels (such as those of Fig. 5). We will discuss the trajectories obtained by our iteration scheme and present a qualitative analysis of the energy and angular dependence of hadronic scattering through the transition region. Only scalar particles will be treated here; the extension to particles with spin is straightforward using the methods described in Refs. 1 and 2.

We turn first to a brief review of large-angle scattering amplitudes. Since we are interested primarily in the nature of the transition between fixed-angle and fixed-t (Regge) behavior, we can utilize the asymptotic large-t and large-u behavior of the scattering amplitude to construct the kernel, K. Thus we shall be able to use the simple asymptotic power-law form of the parton-interchange amplitude. This can be written approximately as

$$K_{AB\to CD} \propto (-s)F_A(-s)F_C(u)F_D(t) \sim s^{1-A}(-u)^{-C}(-t)^{-D}. \tag{17}$$

Here we have assumed the power-law behavior

$$F_I(t) \propto (-t)^I, \quad I = A, B, C, D \tag{18}$$

for the form factors; possible logarithmic factors have been neglected. The above form for K arises when we consider the (ut) parton-interchange diagram of Fig. 6, and particle B has the most convergent form factor. For example, following the naive quark model, we assume that nucleon-nucleon scattering at large angles is controlled by the interchange of the common quarks and for the quark-plus-core bound-state model of the nucleon obtain

$$K_{NN\to NN} \sim s^{-1}(-u)^{-2}(-t)^{-2},$$

where a dipole dependence for the nucleon form factors has been assumed. This result for the scattering amplitude is in excellent agreement with large-angle pp scattering data. Thus if one wishes, one can take the assumed parameterizations of K as simple empirical fits to data, and for most purposes of this paper the theoretical origin can be ignored. However, as we shall discuss later, the identification of K with the interchange amplitude and Reggeization via the hadronic bremsstrahlung mechanism may allow an elegant dynamical interpretation of the Harari-Rosner duality diagrams.[17]

In the case of meson-nucleon scattering, we obtain using (17)

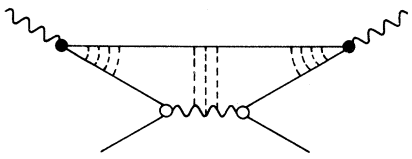

FIG. 5. Example of a dynamical correction to the kernel K which is important at low t, but which is assumed not to be important for large-angle scattering in, for example, the parton-interchange model. The external wavy lines could be hadrons or photons.

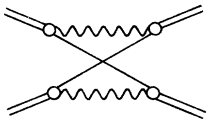

FIG. 6. A (tu) interchange contribution to the kernel, K. The hadrons (double line) are represented at large transverse momentum as parton (solid line) core (wavy line) bound states. The partons do not interact with each other.

$$K_{K^+p\to K^+p}\sim(-u)^{-1}(-t)^{-2}$$

from ($\mathcal{P}$) quark interchange, and the assumption of monopole meson form factors $F_K(t)\sim t^{-1}$ (see also Ref. 18). In the case of $\pi p\to\pi p$ scattering, both the (ut) diagram and the (st) (box) diagram (which are related by s-u crossing) contribute in the quark model. All of these forms, especially the prediction that $d\sigma/dt\sim s^{-8}$ at fixed angle, are consistent with present data. (A complete review is given in Ref. 1.)

To discuss the transition regions, we must discuss the region where $(-u)\sim s$ is large compared to $(-t)$, which may or may not be large compared to a typical squared mass. It is then convenient to write the kernel corresponding to a (ut) parton-interchange diagram as

$$K(u,t)=(\mu^2-u)^{-n}F(t), \tag{19}$$

where

$$n=A+C-1$$

and $F(t)$ falls asymptotically as $(-t)^{-D}$. For example, for p-p elastic scattering, $n\sim 3$ and $D\sim 2$ while for π-p scattering, D is still ~ 2 but $n\sim 1$. [*Note added in proof.* If a 3-quark wave function is assumed for the nucleon, then $n=2$ and $D=2$ for pp scattering. See S. Brodsky and G. Farrar, Phys. Rev. Lett. 31, 1153 (1973).] In a physically realistic consideration of these cases, one must treat a coupled-channel problem, which could include, for example, a dominant $\pi\pi$ channel with $n\sim 1$ and $D\sim 1$. Such a coupled-channel situation will be discussed shortly, but first the simpler single-channel case will be considered. Within the limitations of the models discussed here, this is directly applicable to the transition to Regge behavior arising from the baryon trajectory in backward meson-baryon scattering as illustrated in Fig. 7. For this process $n\sim 2$ and $D\sim 1$.

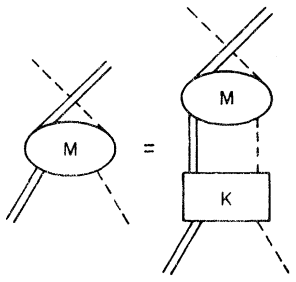

FIG. 7. Integral equation for backward meson-baryon scattering. The double line is a baryon, and the dashed line is a meson.

A. Single-Channel Case

The weight function W for the interchange amplitude of the above form (19) is given by

$$W=\frac{F(t)}{(n-1)!}\,\delta^{(n-1)}(\sigma^2-\mu^2), \tag{20}$$

where $(n-1)$ refers to the derivatives of the δ function. Alternatively, one could impose spectral conditions of $W(\sigma^2,t)$ to achieve the same $(-u)^{-n}$ behavior of K. The dependence of $F(t)$ on the off-shell masses has been neglected. This is permissible in the interchange theory because $F(t)$ is independent of λ^2 and $\tilde{\lambda}^2$ for large enought t and all integrals involved in the equation for M converge rapidly in these off-shell mass variables. (Recall also the discussion of Sec. II.)

Returning to the equation for M, and inserting the above form for W, the σ^2 and ρ^2 integrals can be directly performed and the contribution to M from the second-order iteration of the (ut) graphs is

$$M=(\mu^2-u)^{-n}F(t)+\frac{\pi F^2(t)}{2(2\pi)^3}\,\frac{(2n-1)!}{[(n-1)!]^2}\times\int_0^1 dx\,dy\,d\beta_1 d\beta_2\,\delta(1-x-y-\beta_1-\beta_2)\times(xy)^{n-1}\Delta^{-2n}, \tag{21}$$

where Δ is defined in Eq. (13).

The large-$(-u)$ behavior can be conveniently extracted by standard Mellin-transform techniques (see, for example, the reference in Ref. 19) or, more simply, by noting that only small values of x and y can contribute in this limit and explicitly carrying out their integration. The result is

$$M=(\mu^2-u)^{-n}F(t)\times\left[1+\frac{F(t)\ln(-u/m^2)}{4(2\pi)^2m^{2n}}\int_0^1 dz\,[1+z(1-z)\vec{q}_\perp^{\,2}/m^2]^{-n}\right]. \tag{22}$$

This leads to the identification of the Regge function to this order:

$$\beta(t)=F(t)/\mu^{2n} \tag{23}$$

and

$$\alpha(t)=-n+\frac{\beta(t)(\mu^2/M^2)^n}{4(2\pi)^2}\int_0^1 dz\,[1-z(1-z)t/m^2]^{-n}. \tag{24}$$

We see then that for large $-t$ the trajectory deviates from its asymptotic value of $-n$ ($n>1$) according to

$$\alpha(t) \sim -n + \frac{m^{2(1-n)} F(t)}{2(2\pi)^2 (n-1)(-t)} \,. \tag{25}$$

[If $n=1$, an extra factor of $\ln(-t)$ arises from the z integral.] Thus the rate of approach of $\alpha(t)$ to the value $(-n)$ depends on the falloff of the form factor of particle D. Recall, for example, that πN scattering is characterized by $D \sim 2$.

From Eq. (22) we can also estimate the point at which Regge effects become small compared to the basic interaction term K. This occurs when the second term of M is small compared to the first, i.e., when

$$[\alpha(t)+n]\ln(-u/m^2) \ll 1$$

or

$$(-t/\mu^2)^{1+D} \gg c \ln(-u/m^2) \,. \tag{26}$$

Thus the transition from the deep region, in which only the basic Born term dominates, to the Regge region, where hadronic bremsstrahlung, i.e., iterative effects become important, occurs neither at a fixed value of t nor a fixed angle, but someplace in between. The "softer" the particles involved (that is, the larger the value of D), the smaller the value of $|t|$ required at a fixed value of $(-u)$ for the deep-scattering formulas to be valid.

B. Coupled-Channel Case

In this section we will extend the previous discussion to a coupled-channel situation. A two-channel problem will be set up and solved explicitly but the final matrix forms can be easily extended to any number of channels. The channel labels refer, of course, to the possible two-hadron states of given isotopic spin in the t channel, such as $(\bar{\pi}\pi)$ and $(\bar{p}p)$,[20] which occur in the iteration procedure (see Fig. 8). For simplicity we will assume that power-law falloff in $(-u)$ of the interchange kernel does not depend upon the coupled t-channel states but that the residue does.

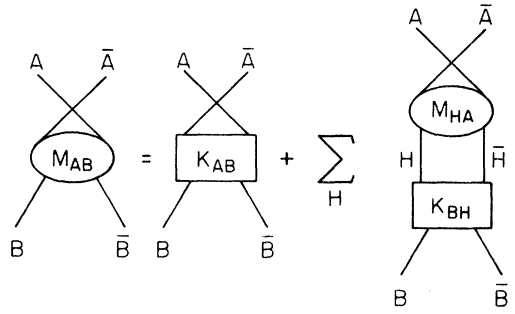

FIG. 8. Full integral equation for the scattering $A+B \to A+B$. The summation over H is over all contributing pairs of hadrons.

Thus if we label the t-channel states by indices i and j, the appropriate weight functions W_{ij}, corresponding to the absorptive parts of the interchange kernels, are assumed to be given by

$$W_{ij} = \frac{F_{ij}(t)}{(n-1)!}\,\delta^{(n-1)}(\sigma^2-\mu^2) + \frac{G_{ij}(t)}{(m-1)!}\,\delta^{(m-1)}(\sigma^2-\mu^2) + \cdots \,. \tag{27}$$

The effects of subsidiary trajectories in the Born terms will be ignored throughout our discussion. More general forms could be considered, for example, μ^2 could depend on i and j, etc., but the above form is sufficient to illustrate the behavior of the leading trajectories and to make the physical points that are of interest here.

Using this W to calculate the scattering matrix to second order, the result coming from the *first term only* in W with equal pairwise masses is

$$M_{ij} = (\mu^2-u)^{-n} F_{ij}(t) + \frac{(2n-1)!}{4(2\pi)^2[(n-1)!]^2} \times \sum_K F_{ik}(t) I_{ij}^k F_{kj}(t) \,, \tag{28}$$

where

$$I_{ij}^k = \int dx\,dy\,d\beta_1 d\beta_2 \delta(1-x-y-\beta_1-\beta_2) \times (xy)^{n-1} (\Delta_{ij}^k)^{-2n} \tag{29}$$

and

$$\Delta_{ij}^k = (1-x-y)M_k^{\,2} + \beta_1\beta_2 \vec{q}_\perp^{\,2} - xyu + (y+x)\mu^2 - x(\beta_1+\beta_2)M_j^{\,2} - y(\beta_1+\beta_2)M_i^{\,2} \,. \tag{30}$$

For large $(-u)$, the asymptotic limit of the integral I_{ij}^k arises from small values of x and y and therefore it does not depend on i or j but only on k. Introducing the diagonal matrix $H(t)$ with elements

$$H_{kk}(t) = \frac{\mu^{2n}}{4(2\pi)^2 (M_k^{\,2})^n} \int_0^1 dz\,[1 - z(1-z)t/M_k^{\,2}]^{-n} \,, \tag{31}$$

the scattering matrix in the limit $(-u) \to \infty$ can be written as

$$M \cong (\mu^2-u)^{-n} \times \left[F(t) + \frac{1}{\mu^{2n}} \ln\left(1-\frac{u}{\mu^2}\right) F(t) H(t) F(t)\right] . \tag{32}$$

In an N-channel situation the scattering matrix will in general be diagonalizable and thus be characterized by N eigenamplitudes. In the large-$(-u)$ limit, each eigenamplitude will have its own independent Regge behavior and residue. Thus, for example, the scattering matrix for two channels will be of the form (neglecting subsidiary trajec-

tories)

$$M=\beta^{+}(t)(-u/\mu^{2})^{\alpha_{+}(t)}+\beta^{-}(t)(-u/\mu^{2})^{\alpha_{-}(t)}, \quad (33)$$

where α_{+} and α_{-} are independent eigentrajectories and β^{+} and β^{-} are (2×2) matrices satisfying the factorization condition

$$\det[\beta^{\pm}(t)]=0. \quad (34)$$

The α's and β's can be determined to lowest order by comparing the Regge expression (33) with the second-order expression (32) for M. One obtains the equations

$$F(t)=\beta^{+}(t)+\beta^{-}(t) \quad (35)$$

and

$$F(t)H(t)F(t)=(\alpha_{+}+n)\beta^{+}(t)+(\alpha_{-}+n)\beta^{-}(t). \quad (36)$$

The trajectory functions are determined from the above equations and the factorization conditions on the residues. The explicit relation that determines the α's is then

$$\det[FHF-(\alpha+n)F]=0. \quad (37)$$

The roots of this equation are the eigentrajectories. In the two-channel case under discussion, the trajectories are given by

$$2(\alpha_{\pm}+n)=\mathrm{Tr}FH\pm[(\mathrm{Tr}FH)^{2}-4\det FH]^{1/2}. \quad (38)$$

The residues can then be written as

$$\beta^{\pm}(t)=\pm[\alpha_{+}(t)-\alpha_{-}(t)]^{-1}[FHF-(\alpha_{\mp}+n)F]. \quad (39)$$

The most important feature of the solution to note at this point is that both eigentrajectories have the same asymptotic limit, $\alpha_{\pm}(-\infty)=-n$. This, of course, is a direct consequence of the fact that the trajectories and residues must be such as to reproduce the Born terms, i.e., interchange kernels, at large momentum transfer. Since the Born term does not in general factorize, more than one Regge pole is necessary to allow this limiting behavior while simultaneously satisfying the factorizability requirements on the trajectory residues. It should also be noted that the scattering matrix for the cases considered so far is purely real, so that when we speak of a Regge trajectory we really mean a strongly exchange-degenerate pair of trajectories added together with the sign appropriate to a purely real contribution. The effects of signature will be discussed later.

We are now finally in a position to discuss the most realistic case: that of the coupled t-channel $\bar{\pi}\pi$ and $\bar{p}p$ systems, in which the power falloff of the interchange kernels is not all the same. In this case the two coupling matrices, F and G in Eq. (27) are required to be nonzero. Fortunately, the discussion of Reggeization is in lowest order only slightly more complicated since the cross terms between F and G do not generate a $\ln(-u)$ behavior in the second-order calculation. The cross-term integrals produce a contribution to M which in leading order has the simple form

$$\frac{1}{(m-n)}[C(m,n,t)(\mu^{2}-u)^{-n}-C(n,m,t)(\mu^{2}-u)^{-m}].$$

That is, the integral reproduces the behavior of the basic Born terms if $m\neq n$, but yields the logarithmic contribution necessary for Regge behavior if $m=n$. As follows from the previous discussion, the trajectories that approach $(-n)$ and $(-m)$ are each doubled in the general case.

In the physically interesting $\bar{\pi}\pi$ and $\bar{p}p$ coupled-channel system, recall that the interchange theory (which agrees well with experiment) predicts asymptotically that

$$\begin{aligned} &n\sim1:\ F_{22}=0,\ F_{11}\sim(-t)^{-1},\ F_{12}=F_{21}\sim(-t)^{-2};\\ &m\sim3:\ G_{22}(-t)^{-2},\ G_{11}=G_{12}=G_{21}=0. \end{aligned} \quad (40)$$

The label 1 refers to the $\bar{\pi}\pi$ channel and 2 refers to the $\bar{p}p$ channel. Of particular interest here is the manner in which M_{22} makes the transition from the Regge region to the deep region. The two leading Regge trajectories, both of which approach $(-n)$ asymptotically, must cancel in this amplitude. Using our previous results the trajectories are given by

$$\alpha_{\pm}=-n+\tfrac{1}{2}[F_{11}H_{11}\pm(F_{11}{}^{2}H_{11}{}^{2}+4H_{11}H_{22}F_{12}{}^{2})^{1/2}]. \quad (41)$$

For large momentum transfer they approach their asymptotic limits as

$$\begin{aligned} &\alpha_{+}\sim-n+H_{11}F_{11}\sim-n+O(-t)^{-2},\\ &\alpha_{-}\sim-n-H_{22}F_{12}{}^{2}/F_{11}\sim-n-O(-t)^{-4}, \end{aligned} \quad (42)$$

and thus α_{-} is much flatter than α_{+}. The residues for the 22 process ($pp\to pp$) behave for large $(-t)$ as

$$\beta_{22}^{+}=-\beta_{22}^{-}=H_{11}F_{12}{}^{2}(\alpha_{+}-\alpha_{-})^{-1}\sim F_{12}{}^{2}/F_{11}\sim(-t)^{-3}. \quad (43)$$

The lower-lying trajectory (which is not doubled in this order) approaches $-m$ for asymptotic $(-t)$ and behaves as

$$\alpha_{0}(t)\sim-m+H_{22}F_{22}\sim-m+O(-t)^{-3}. \quad (44)$$

Thus as $(-t)\to\infty$, M_{22} has the behavior

$$M_{22}=\beta_{22}^{+}\left[\left(\frac{-u}{\mu^2}\right)^{\alpha_+}-\left(\frac{-u}{\mu^2}\right)^{\alpha_-}\right]+G_{22}\left(\frac{-u}{\mu^2}\right)^{\alpha_0(t)}$$

$$\sim H_{11}F_{12}{}^{2}\frac{\ln(-u/\mu^2)}{(-u)^n}+\frac{G_{22}}{(-u)^m}[1+H_{22}G_{22}\ln(-u/\mu^2)]$$

$$\sim\frac{\ln(-u/\mu^2)\ln(-t/\mu^2)}{(-t)^5(-u)}+\frac{1}{(-t)^2(-u)^3}\left[1+\frac{\ln(-u/\mu^2)}{(-t)^3}\right]. \tag{45}$$

Thus the nonleading Regge trajectory dominates in the fixed-angle, deep region by almost a full power of s because the two leading trajectories cancel. For small $|t|$, however, it is clear that the trajectory α_+ dominates the scattering amplitude for all coupled processes. Since α_+ arises primarily from the pion channels in the iterative process, we can rephrase this result as implying that all hadron-hadron beams are essentially pion beams at large impact parameters. That is, in the region of small $|t|$ or $|u|$, incoming hadrons produce pions in a bremsstrahlung process (the bremsstrahlung spectrum being characterized by Regge behavior); these pions then undergo the basic interchange interactions. Note that coherent Regge effects become unimportant and the Born term dominates when

$$\frac{(-t)^3}{(-u)^2}\gg\mu^2 c\ln\left(\frac{-u}{\mu^2}\right)\ln\left(\frac{-t}{\mu^2}\right). \tag{46}$$

This is to be compared with Eq. (26) for the single-channel case.

C. Signature

In our discussions so far, we have limited ourselves to cases in which the irreducible kernels have discontinuities in u for positive u, but no discontinuities in s for positive s. As a result of this restriction, the amplitudes generated by t-channel iterations of these irreducible kernels have been purely real. In Regge language, this means that we have been generating only pairs of strongly exchange-degenerate Regge poles. In general, however, hadronic amplitudes are not purely real, and so we must generalize our Reggeization procedure to include the possibility of nonzero imaginary parts. The imaginary parts of amplitudes described by Regge poles come from the rotating phase terms of the signature factors, and so the generalization to complex amplitudes requires a method of properly including signature factors in the Regge poles. This is the task of the present section.

To see how signature factors come about in our scheme, consider the simple one-channel problem defined by specifying the basic interaction

$$K=f(t)(\mu^2-s)^{-n}. \tag{47}$$

This represents a Born amplitude which has singularities for $s>0$. Since $t\leq 0$, we need not concern ourselves with any of the singularities in t. In the parton-interchange model, such a Born term corresponds to an (st) interchange graph. We now want to iterate this kernel in the t channel. Using the notation of Fig. 9, we can write

$$M_1=\frac{f^2(t)}{(n-1)!\,2(2\pi)^4}\int_{-\infty}^{\infty}\frac{dy\,d^2l_\perp dl^2}{2|y|}\,d\sigma^2[l^2-m^2+i\epsilon]^{-1}$$
$$\times[(l+q)^2-m^2+i\epsilon]^{-1}$$
$$\times[(p+l+q)^2-\sigma^2+i\epsilon]^{-1}$$
$$\times[(l+q+r)^2-\mu^2+i\epsilon]^{-n}$$
$$\times\delta^{(n-1)}(\mu^2-\sigma^2), \tag{48}$$

where we have used the dispersion representation

$$f(t)(\mu^2-s)^{-1}=\frac{f(t)}{(n-1)!}\int d\sigma^2\frac{\delta^{(n-1)}(\sigma^2-\mu^2)}{s-\sigma^2+i\epsilon}$$

for the lower amplitude. The upper external lines of Fig. 9 are uncrossed since K has a singularity for $s>0$, rather than $u>0$. The s variables for the lower and upper subamplitudes are, respectively, $s'=(p+l+q)^2$ and $\bar{s}=(l+q+r)^2$. The expression for M_1 can be evaluated by methods similar to those used before. In the present case, the only nonzero contributions to the integral come from the region $-1<y<0$. For our purposes, however, it is easier to simply shift the origin of the d^4l integration. With the substitution $l\to -l-q$, it is clear that (48) is identical to (11). In particular, therefore, the asymptotic behavior of (48) for $|u|\to\infty$ (or $s\to\infty$) is

$$f^2(t)H(t)(\mu^2-u)^{-n}\ln(-u) \tag{49}$$

as in (32). This result can be understood by drawing Feynman diagrams in, say, ϕ^3 theory. In that case, it is easy to see that the t-channel iteration

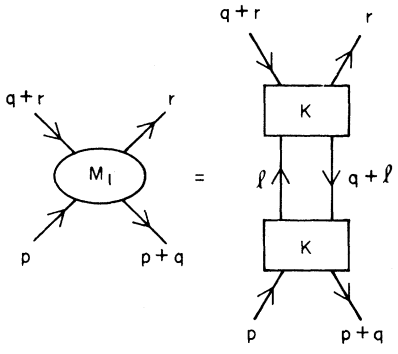

FIG. 9. Labeling of the integral equation for the first iteration of K. The equation gives the first correction to the asymptotic values of the effective trajectories. The top lines are uncrossed here since these diagrams are planar in the s-t plane.

of two s-channel poles has the same topology as the t-channel iteration of two u-channel poles. [Recall that because of our conventions, it is necessary to cross the intermediate lines to keep the quantum numbers flowing properly, and this results in an over-all nonplanar graph with (ut) topology.]

Now, suppose we wish to continue iterating the kernel. The third-order iteration presents us with a new situation; the kernel has an s-channel (i.e., positive s) discontinuity, but the amplitude M_1, with which it is convoluted, has a u-channel discontinuity. Using arguments similar to those sketched above, one can show that this graph is related to the third-order graph calculated by iterating three times a (ut) Born term by $s \leftrightarrow u$ crossing. In particular, the leading term as $s \to \infty$ is

$$M_2 = f^3(t)H^2(t)(\mu^2 - s)^{-n} \ln^2(-s)/2! \ .$$

Furthermore, the same result follows from the convolution of a kernel which has a u-channel discontinuity with a subamplitude M_1, which has an s-channel discontinuity. These topological properties are conveniently summarized by the following rules:

$$u \otimes u = u,$$

$$s \otimes s = u,$$

$$s \otimes u = s,$$

$$u \otimes s = s.$$

Here $u(s)$ stands for any amplitude with only a u-channel (s-channel) discontinuity, and $\otimes$ denotes the operation of convolution. We remark in passing that kernels which have discontinuities both for $u > 0$ and $s > 0$ (su) amplitudes can be handled in a similar way. These kernels have nonzero third double-spectral functions and correspond, for example, in the parton-interchange theory, to (su) interchange graphs. When such a kernel is inserted as a subamplitude into our recursion relation, it generates an output amplitude with both s- and u-channel discontinuities. The topology rules for (su) amplitudes are

$$su \otimes u = s \otimes u + u \otimes u = s + u,$$

$$su \otimes s = s \otimes s + u \otimes s = u + s,$$

$$su \otimes su = s \otimes s + s \otimes u + u \otimes s + u \otimes u$$
$$= s + u.$$

Let us return now to the problem posed at the beginning of this section. To see the structure of the total amplitude M, generated by iterations of the Born term (47), it is convenient to use a (perturbation) approximation keeping only the highest powers of $\ln(-u)$ or $\ln(-s)$ coming from each order of the iteration. It is then a simple matter to sum these terms. The result is

$$M = \tfrac{1}{2} f(t)[(-u)^{\alpha_+} + (-s)^{\alpha_+}]$$
$$- \tfrac{1}{2} f(t)[(-u)^{\alpha_-} - (-s)^{\alpha_-}], \qquad (50)$$

where $\alpha_\pm(t) = -n \pm f(t)H(t)$ in this approximation. We therefore have two nonexchange degenerate, signatured Regge poles of opposite signature. For $|t| \to \infty$, $\alpha_\pm(t) \to -n$ and the trajectories do become degenerate, their sum reproducing the Born term as required by consistency. As we move to smaller $|t|$, however, the trajectories split, one rising while the other falls. This is to be contrasted with the case in which the kernel has only a u-channel discontinuity. In that case, we can also write the amplitude as the sum of two signatured Regge poles, but they must be exactly strongly exchange-degenerate. The fact that the residues of the poles in (50) are (up to a sign) equal is an artifact of our approximation. This equality will be broken by the terms we have neglected in deriving the above expression (50).

The results we have been discussing depend only on the singularity structure of the kernels used in the iteration scheme. If we apply our methods to the parton-interchange theory, we find that iterations of (tu) graphs generate pairs of exchange-degenerate poles, while the iterations of (st) graphs generate pairs of non-exchange-degenerate poles. There is evidently a correspondence between these observations and the predictions of Harari-Rosner duality diagrams.[17] In the case of duality diagrams, a $2 \to 2$ hadronic scattering amplitude with exotic s-channel quantum numbers is represented by a nonplanar diagram which, for forward (elastic) scattering generally looks like a (tu) parton-interchange diagram. The nondiffractive parts of such amplitudes are predicted to be real in the Regge region, i.e., the leading non-Pomeron Regge poles are supposed to be exchange-degenerate near $t = 0$. On the other hand, planar duality diagrams which look just like (st) parton-interchange diagrams can be drawn for reactions with nonexotic s- and t-channel quantum numbers. For such amplitudes exchange degeneracy among the non-Pomeron poles near $t = 0$ is not expected. The same rules of exoticity that determine whether or not a planar duality diagram can be drawn also determine if a planar parton-interchange diagram can be drawn. In the single-channel case, therefore, there is a straightforward connection between the predictions of duality diagrams near $t = 0$ and parton-interchange diagrams in the deep region, since t-channel iterations of the (tu) interchange amplitude generate pairs of exchange-

degenerate poles, while no such degeneracy automatically follows from the iteration of (st) interchange amplitudes.

In the more realistic coupled-channel problem, the correspondence is not quite so simple, since planar (st) subamplitudes will in general contribute in the iteration scheme to processes with exotic s-channel quantum numbers, and thus will generate imaginary parts in such amplitudes. However, these imaginary parts, in addition to contributing to very low-lying trajectories, probably build the Pomeron pole. In fact, in the context of our Reggeization scheme, a quite natural characteristic of the Pomeron pole is that it is a measure of how much the particles entering the bottom of the graph forget their identity on their way up the ladder.[19] (See the discussion for further clarification.)

V. DISCUSSION

It is a well-known and obvious fact that the sum of simple ladder graphs yields an amplitude which is Regge behaved. In this paper we have derived a particularly useful form of the integral equation describing such graphs which can also handle generalized ladder graphs. This equation was used to extract the limiting behavior of the Regge functions in the case of general input Born terms of physical relevance in both the single- and coupled-channel situations.

In this latter case, it was shown that if the basic Born terms do not factorize (i.e., if they are not of rank one—which is certainly the situation in general) then multiple eigen-Regge trajectories are generated which have the property that they become degenerate asymptotically. This happens in such a way that the sum of the separate Regge contributions, each of which factorizes, correctly reproduces the nonfactorizing input terms. Thus it is expected that such degeneracies will be a quite common phenomenon if the basic input terms have the general structure used here.

In the physical example of the coupled meson-baryon system which was briefly discussed in the text, we expect the leading and most important trajectories to be roughly as shown in Fig. 10 for each signature. The input to this calculation is a fit to elastic πp and pp scattering at large angles based on the interchange model,[1] which is in agreement with the phenomenological analysis of the effective Regge trajectory for the above processes.[21] In a calculation which includes the effects of signature, this model also predicts that in p-p scattering the nonleading, but surviving, trajectories rapidly become exchange degenerate as $|t|$ increases and both approach α_0.

Some general predictions following from this approach which are in addition to the specific limiting behavior derived in the text are:

(1) For any process, the existence of hadronic bremsstrahlung will lead to Regge behavior at small momentum transfers. As $|t|$ increases, this multihadronic component of the wave function will become less important and the basic interaction mechanism will increase in importance. The physical reason for this is that if the basic interaction falls with energy, then a high-energy projectile will prefer to emit hadrons (via a bremsstrahlung-type process) which have less longitudinal momentum and hence can interact at a lower effective energy. At large $|t|$ values, it is difficult for this emitted particle to be reabsorbed by the projectile as required for an elastic or quasielastic scattering process. At low $|t|$ values, however, reabsorption can occur easily, and this leads to the Reggeization of the amplitude which should control the behavior of the process in this kinematic region.

(2) The above theory of Regge behavior in exclusive scattering is physically the same as that described in Ref. 2 for the inclusive case. However, it is interesting to note the contrast between the mechanisms that suppress Regge behavior at large transverse momentum in exclusive scattering and in the pionization region of inclusive scattering. In the exclusive case, it is the fact that at large momentum transfer, the probability of reabsorbing all the hadronic bremsstrahlung is small. In the inclusive case, it is energy-momentum conservation—the radiated hadron that is responsible for directly producing the detected particle must have the necessary energy and momentum.

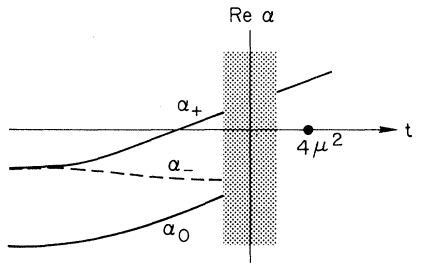

FIG. 10. Regge trajectories of hadronic scattering. The α_+ and α_- trajectories become degenerate at -1 for $t \to -\infty$ and control large-angle meson-baryon scattering. The $\alpha_\pm$ trajectories cancel in baryon-baryon scattering exposing the α_0 trajectory which is expected to approach -3 at $t \to -\infty$ in the interchange theory. Although the iteration scheme becomes very complicated to compute for $t \sim 0$, the trajectories are expected to smoothly continue to positive t, where at least some of them will be associated with physical hadrons according to the usual dicta of Regge theory.

(3) For sufficiently large but fixed t, the $\pi\pi$ and πp differential cross section should have an energy dependence corresponding to a trajectory having the value $\alpha(t) \sim -1$. Furthermore, if the parton-interchange picture is correct, the associated residues $\beta(t)$ should fall in t as the pion and nucleon form factors, respectively.

(4) In general, we expect the $I=0$ and $I=1$ exchanges to have the same limiting trajectory value and residue behavior. It is possible to adjust the hadronic wave functions to destroy this expected degeneracy, but this would not be a very natural choice.

(5) As was pointed out in Ref. 21, the fact that the large-angle behavior of the amplitude is related to the asymptotic behavior of the Regge trajectories yields relations between *a priori* unrelated Regge functions.[22] For example, in meson-nucleon scattering, as one moves out from the forward direction, the exchange meson trajectories must join smoothly on to the basic interaction describing the 90° behavior. Similarly, as one moves out from the backward direction, the exchanged baryon trajectories and residues must join smoothly on to the same 90° amplitude. Thus, the baryonic trajectories and residues are related to the mesonic residues and trajectories at large momentum transfer.

(6) For sufficiently large $|t|$, the pp scattering amplitude should become exchange degenerate without subtracting out the Pomeron contribution since it is most naturally associated with the leading trajectories which cancel for large $|t|$.[19]

(7) The complexities in our calculational approach near zero momentum transfer arise from two sources. The fact that there is a trajectory near 1 means that unitarity in the s and u channels must be taken care of properly. The second point is that the two-hadron irreducible kernels K were approximated by forms which should be accurate and relevant only for large $|t|$ values. Therefore the output could hardly be trusted for small t values. It is certainly natural to assume, however, that the trajectories we compute for large negative t will continue to positive t and in some sense keep their identity (except perhaps for the leading $I=0$ Pomeron singularity which goes to 1 at $t=0$) thus giving rise to particles and resonances.

(8) There seems to be an intriguing parallel between the interchange graphs iterated in the t-channel and duality diagrams, as we discussed at the end of Sec. IV. Perhaps we can make this relationship somewhat clearer by drawing an analogy from atomic physics.

Consider the problem of an atom in a magnetic field. For zero external field, all the states with a given J (total angular momentum) have very nearly the same energy and are thus degenerate. When a weak magnetic field is applied, the $(2J+1)$ degenerate states split, and we have the Zeeman effect. As the external field is increased, the energy levels of states with different J and M_J change, until finally in a very strong field some of the levels again become degenerate (the Paschen-Back effect). The degeneracy pattern for a strong field is, however, not the same as the degeneracy pattern for the weak field. The reason is that different pieces of the Hamiltonian are dominant in the two different regions, and so the approximate eigenstates of the Hamiltonian are not the same. Exactly the same thing happens in hadronic scattering. In the deep region ($|t| \to \infty$), a number of Regge trajectories become degenerate as we have shown. This is because, in this domain, the most important forces are those which are short-ranged. In the Regge region, we again find degeneracy among various trajectories, but here the degeneracy arises because the long-range part of the Hamiltonian is most important (large impact parameters), and so the approximate eigenstates are different. In the single-channel case the degeneracy patterns are simple enough so that the connection between duality diagrams and parton-interchange diagrams can be easily made. But a realistic coupled-channel situation involves many trajectories so that the exact relationships among them over the entire t range is complicated, indeed. Nevertheless, the analogy presented here shows why one should expect degeneracies among trajectories at large $|t|$ and in general, a different degeneracy pattern at small $|t|$.

(9) Our experience in fitting the lowest-order predictions of the interchange theory to experimental data leads us to expect that the type of behavior predicted here for the transition region will improve both the fit to the data and extend the range over which a fit can be carried out. The rather striking cancellation between the leading trajectories in pp scattering and the degeneracy of the leading trajectories in the πp case should produce effects which can be clearly seen experimentally. These effects may have been responsible for some of the difficulties found in attempts to extend simple Regge fits to higher momentum transfer.

In this paper we have tried to accomplish two main objectives. The first has been to derive an integral equation which allows a simple discussion of Regge behavior arising from generalized ladder-type interactions. The second has been to apply this equation by considering a basic interaction which correctly reproduces the features of large-angle data and which has some theoretical motiva-

tion. Thus we have gone considerably beyond the normal Regge approach to scattering by predicting the behavior of trajectories (their asymptotic limit and the approach to that limit), and the behavior of their residue functions at large momentum transfer. We cannot extend these predictions to small t values without considerably expanding the input assumptions and the dynamics.

The general behavior of the trajectories arising from our model is in good agreement with the effective trajectories derived from experiment in Ref. 21. However, the cancellation between the leading trajectories in pp scattering is a rather novel effect which will require considerably more experimental confirmation. Its existence depends on the fact that the meson-nucleon and nucleon-nucleon differential cross sections fall with a different power of the energy at fixed, large angle. This does seem to be the case in the present experimental regime.

While a full comparison with experiment of a Regge parameterization of the type proposed here has not yet been carried out, the success of the fits described in Ref. 1 and the trend of the fits at smaller momentum transfer lead us to expect good agreement.[23] This would considerably extend the applicability in a new kinematical direction of a type of theory which has already been successfully applied to reactions ranging from pion-nucleon scattering at ≈ 5 GeV/c to the inclusive production of large-transverse-momentum mesons at the CERN ISR.[24]

APPENDIX

In this appendix we give an alternate derivation of the basic iterative equation (10), given in the text, for the case of (generalized) ladder graphs. Time-ordered perturbation theory in the infinite-momentum frame of Eq. (4) will be used.[25] The momenta of the internal particles are defined in the text and, as before, ν^2 and ν'^2 are the masses of the lower external particles. The advantage of choosing a frame in which the upper two particles do not carry any longitudinal momenta is that only the trapezoidal time-ordered graph of Fig. 2 contributes.

Defining E_J to be $2P$ times the energy of the intermediate state J, the required "energy" denominators are of the form $D_J = E - E_J$. For example, the first denominator on the left is

$$D_N = \nu^2 - \frac{\vec{l}_N^{\,2} + M^2}{x_N} - \frac{\vec{l}_N^{\,2} + \mu^2}{1 - x_N} \equiv \nu^2 - S(\vec{l}_N, x_N) . \tag{A1}$$

(For convenience we drop the $\perp$ subscript on all transverse momenta.) The second denominator is conveniently written in the form

$$D_{N-1} = D_N + E_N - E_{N-1} = D_N + \frac{1}{x_N}\left[M^2 - S(\vec{l}_{N-1} - x_{N-1}\vec{l}_N, x_{N-1})\right] .$$

In general

$$D_J = D_N + \frac{1}{\omega_N}\left[M^2 - S(l_{N-1} - x_{N-1}l_N, x_{N-1})\right] + \frac{1}{\omega_{N-1}}\left[M^2 - S(l_{N-2} - x_{N-2}l_{N-1}, x_{N-2})\right] + \cdots + \frac{1}{\omega_{J+1}}\left[M^2 - S(l_J - x_J l_{J+1}, x_J)\right] , \tag{A2}$$

where

$$\omega_J = x_N x_{N-1} \cdots x_J .$$

The central energy denominator takes the form

$$D_0 = D_1 + \frac{1}{\omega_1}\left[l_1^2 - (l_1 - r)^2\right] - 2p \cdot r = u + r_\perp^{\,2} - \nu^2 + D_1 + \frac{1}{\omega_1}\left[l_1^2 - (l_1 - r)^2\right] , \tag{A3}$$

which is actually independent of ν^2 at fixed u. The denominators on the right-hand side of the diagram have the form

$$D_N^q = E - E_N' = \nu'^2 - S(l_N + (1 - x_N)q, x_N) ,$$

$$D_{N-1}^q = D_N^q + \frac{1}{\omega_N}\left[M^2 - S(l_{N-1} + (1 - x_{N-1})q, x_{N-1})\right] .$$

Thus the $(N+1)$th-order ladder contribution to the scattering amplitude is simply

$$M_{N+1} = \left(\frac{g^2}{2(2\pi)^3}\right)^{N+1} \times \int \prod_{i=1}^{N}\left[\frac{d^2 l_i dx_i}{(x_i)^{1+2i}(1 - x_i) D_i D_i^q}\right]\frac{1}{D_0} , \tag{A4}$$

where g is the coupling constant describing the three-particle vertices.

An iterative form for this equation can be derived by writing down a similar formula for M_{N+2}, changing variables in it from l_J to l_J' defined by

$$l_J' - x_J l_{J+1}' = l_J - x_J l_{J+1}$$

for $J = 1, 2, \ldots, N-1$, and

$$l_N' = l_N - x_N l_{N+1} , \qquad l_{N+1} = k , \quad x_{N+1} = x , \tag{A5}$$

and comparing to (A4). We find

$$M_{N+2}(u,-q^2;\nu^2,\nu'^2,-r^2,-(q+r)^2)$$
$$=\frac{g^2}{2(2\pi)^3}\int\frac{d^2k\,dx}{x^2(1-x)DD^q}\times M_{N+1}(u',-q^2;\lambda^2,\lambda'^2;-r^2,-(q+r)^2)\,, \tag{A6}$$

where

$$D=\nu^2-S(k,x),\quad \lambda^2-M^2=xD\,,$$
$$D^q=\nu'^2-S(k+(1-x)q,x),\quad \lambda'^2-M^2=xD^q\,, \tag{A7}$$

and a rearrangement of D_0 shows that we must define u' by

$$u'-M^2=x[u-S(k-(1-x)r,x)]\,. \tag{A8}$$

The integral equation for the full ladder scattering amplitude is then

$$M(u,-q^2;\nu^2,\nu'^2;-r^2,-(q+r)^2)$$
$$=B+\frac{g^2}{2(2\pi)^3}\int\frac{d^2k\,dx}{x^2(1-x)DD^q}\times M(u',-q^2;\lambda^2,\lambda'^2;-r^2,-(q+r)^2)\,, \tag{A9}$$

with

$$B=g^2(\mu^2-u)^{-1}\,. \tag{A10}$$

The generalized folding formula (10) of the text can be derived after only slightly more work by treating as a unit the addition of two (or more) rungs to the ladder.

---

*Work supported by the U. S. Atomic Energy Commission.

†Present address: Dept. of Physics, University of Pittsburgh, Pittsburgh, Pennsylvania 15260.

‡Present address: National Accelerator Laboratory, Batavia, Illinois 60510.

[1]J. F. Gunion, S. J. Brodsky, and R. Blankenbecler, Phys. Lett. 39B, 649 (1972); Phys. Rev. D 8, 287 (1973). The latter reference furnishes details concerning the infinite-momentum-frame bound-state wave-function formalism. These papers concentrate on applications to exclusive processes of the interchange theory.

[2]J. F. Gunion, S. J. Brodsky, and R. Blankenbecler, Phys. Rev. D 6, 2652 (1972); R. Blankenbecler, S. J. Brodsky, and J. F. Gunion, Phys. Lett. 42B, 461 (1973). These papers apply interchange concepts to inclusive reactions.

[3]J. F. Gunion, Report No. MIT-CTP-346, presented at the Vanderbilt Conference, 1973 (unpublished).

[4]H. Fried and T. Gaisser, Phys. Rev. D 4, 3330 (1971); H. Moreno, *ibid.* 5, 1417 (1972).

[5]S. M. Berman, J. D. Bjorken, and J. B. Kogut, Phys. Rev. D 4, 3388 (1971).

[6]D. Horn and M. Moshe, Nucl. Phys. B48, 557 (1972).

[7]J. Harte, Phys. Rev. 189, 1936 (1969).

[8]R. Blankenbecler, S. Brodsky, J. Gunion, and R. Savit (to be published).

[9]R. P. Feynman, Phys. Rev. Lett. 23, 1415 (1969).

[10]S. J. Chang and S. K. Ma, Phys. Rev. 180, 1506 (1969).

[11]M. Schmidt, SLAC Report No. SLAC-Pub-1265, 1973 (unpublished).

[12]One must be careful when interchanging the orders of integration with this variable change; extra $\delta(x)$ contributions can occur if the integrands are functions of l^2 only. These extra contributions do not occur in our applications. See S. Brodsky, R. Roskies, and R. Suaya, SLAC Report No. SLAC-PUB-1278, 1973 (unpublished), and T. Yan, Phys. Rev. D 7, 1780 (1973).

[13]The deformation of the σ^2 line integral is due to the interchange of the order of integration and is similar to that found in a discussion of anomalous thresholds. See R. Blankenbecler, M. L. Goldberger, S. W. MacDowell, and S. B. Treiman, Phys. Rev. 123, 692 (1961).

[14]Because we have chosen a Born term with only a u-channel discontinuity, all the graphs generated by iteration of this term will be nonplanar, and the entire amplitude obtained by summing these ladders will be real. This means that the Regge poles generated by the sum will lack signature factors—more properly, this ladder series will generate a pair of strongly exchange-degenerate poles, whose rotating phase parts cancel. We shall discuss the effects of signature in Sec. IV C.

[15]B. W. Lee and R. F. Sawyer, Phys. Rev. 127, 2266 (1962).

[16]See R. J. Eden, P. V. Landshoff, D. I. Olive, and J. C. Polkinghorne, *The Analytic S-Matrix* (Cambridge University Press, New York, 1966). This has also been discussed in the infinite-momentum frame by J. B. Kogut, Phys. Rev. D 4, 3101 (1971).

[17]H. Harari, Phys. Rev. Lett. 22, 562 (1969); J. L. Rosner, *ibid.* 22, 689 (1969). P. G. O. Freund, Nuovo Cimento Lett. 4, 147 (1970).

[18]G. Barbiellini *et al.* and V. Alles-Borelli *et al.*, reported by V. Silverstrini, in *Proceedings of the XVI International Conference on High Energy Physics, Chicago-Batavia, Ill., 1972,* edited by J. D. Jackson and A. Roberts (NAL, Batavia, Ill., 1973), Vol. 4, p. 1.

[19]A simple argument which supports this interpretation may be found in R. Savit, SLAC report and Ph.D. thesis, Stanford University, 1973 (unpublished).

[20]Here we use the term pion as a label for all mesons having essentially monopole form factors and the term proton for all baryons with dipole form factors. We shall not keep track of either strangeness or isospin.

[21]Tran Thanh Van, D. D. Coon, J. F. Gunion, and R. Blankenbecler (unpublished).

[22]Relations of the type described here, as well as a number of other asymptotic conditions on Regge param-

eters have been derived from a more general point of view which does not rely on the specific Reggeization scheme discussed here. R. Savit and R. Blankenbecler (unpublished).

[23]The coherent sum of Regge poles plus the Born interchange amplitude has been used by A. Donnachie and P. R. Thomas to fit backward pion-nucleon scattering and nucleon pair annihilation into mesons [Daresbury Reports Nos. DNPL/P166 and DNPL/149, 1973 (unpublished)]. This type of model fits very naturally into the predictions of this paper, where one characteristically expects a normal leading Regge trajectory plus a nonleading Regge trajectory plus a nonleading one which remains near and just below the input interchange value and hence could be approximately given by the interchange amplitude itself with a different over-all strength.

[24]F. W. Busser *et al.*, CERN report (unpublished).

[25]S. Weinberg, Phys. Rev. 150, 1313 (1966).

PHYSICAL REVIEW D VOLUME 8, NUMBER 11 1 DECEMBER 1973

Saturation of Chiral SU(2) ⊗ SU(2) Algebras, $A_1\rho\pi$ and ρ' Couplings

Seisaku Matsuda
Department of Physics, Polytechnic Institute of Brooklyn, Brooklyn, New York 11201

C. Y. Huang* and S. Oneda*
Center for Theoretical Physics, Department of Physics and Astronomy, University of Maryland, College Park, Maryland 20742

(Received 25 June 1973)

The interrelation between the two different types of sum rules, the chiral SU(2) ⊗ SU(2) spectral-function sum rules and the ones based on the saturation of the chiral SU(2) ⊗ SU(2) charge algebras (which also includes the time derivative of axial-vector charge) especially studied by Gilman and Harari (G-H), is investigated through the charge-charge density algebras and under the *same* single-particle approximation. It is shown that, if the ρ meson is the only $I = 1$ vector meson, (i) the G-H saturation is justified for the case of helicity $\lambda = 0$, (ii) the whole set of sum rules is entirely consistent with each other, including the second-spectral-function sum rules, and (iii) $m_A^2 \simeq 2m_\rho^2$ thus follows to the extent that the KSRF (Kawarabayashi-Suzuki-Riaduddin-Fayyazuddin) relation is experimentally satisfied. The modification due to the addition of the newly discovered ρ' meson to the scheme is studied. It is found that the ρ' cannot play a dominant role and its relevant couplings, $\rho'\pi\pi$ and ρ'-γ, are restricted to small values. Typically, we obtain $\Gamma(\rho' \to \pi\pi) \simeq 50$–$80$ MeV and $(G_{\rho'}/G_\rho)^2 \simeq 0.2$, if the ρ' is treated as the triplet D states of the quark model and no more vector mesons are introduced. Some remarks are also made about the $A_1\rho\pi$ coupling.

I. INTRODUCTION

Whether the A_1 mass agrees with the prediction[1] $m_A = \sqrt{2}m_\rho$ or not is still controversial. The Particle Data Group[2] lists its mass around 1070 MeV but with the comment[2,3]—broad enhancement in the $J^P = 1^+$ $\rho\pi$ partial wave; not a Breit-Wigner resonance. Some say[4] that it is a broad effect centered at (presumably) higher mass. On the other hand, considerable evidence (but again not clearcut) also exists for the possible SU(3) counterparts of A_1, i.e., $K_A(1240)$, $D(1285)$, $E(1422)$, etc.

There is also now convincing evidence[3] for the existence of another ρ meson called ρ' ($\rho' \to \rho^0\pi^+\pi^-$, with $M \simeq 1.5$ GeV and $\Gamma \simeq 0.4$ GeV). It could, for example, be the triplet D states of the quark model. One of the interesting problems related to the ρ' is the strength of the $\rho' \to \pi\pi$ and ρ' photon couplings. The other is the effect of the ρ' on the sum rules involving ρ, A_1, and π mesons, etc. We study these problems in close connection with the earlier works based on the chiral SU(2)⊗SU(2) algebras.

Define G_ρ, G_A, and F_π by $(2q_0)^{1/2}\langle 0|V_\mu^\pi(0)|\rho^-(\vec{q})\rangle = G_\rho \epsilon_\mu^\rho$, $(2q_0)^{1/2}\langle 0|A_\mu^{\pi^+}(0)|A_1^-(\vec{q})\rangle = G_A\epsilon_\mu^A$, and $(2q_0)^{1/2} \times \langle 0|A_\mu^\pi(0)|\pi^-(\vec{q})\rangle = F_\pi q_\mu$, respectively [$V_\mu^\pi(x) = V_\mu^1(x) + iV_\mu^2(x)$, $A_\mu^\pi(x) = A_\mu^1(x) + iA_\mu^2(x)$, etc.].

From the spectral representation of the vacuum expectation values of the currents $V_\mu^i(x)$ and $A_\mu^i(x)$ or the algebra of the gauge fields, Weinberg[1] obtained the spectral-function sum rules,[5]

$$\frac{G_\rho^2}{m_\rho^2} - \frac{G_A^2}{m_A^2} = F_\pi^2 \quad \text{(first sum rule)}, \tag{1}$$

$$G_\rho^2 = G_A^2 \quad \text{(second sum rule)}. \tag{2}$$

Das, Mathur, and Okubo[6] also obtained these sum rules by requiring that leading terms in the asymptotic expansion of the current propagators become SU(2)⊗SU(2) invariant at high momenta.

The so-called KSRF relation[7]